Article

Characterization of Polyelectrolyte Complex Formation Between Anionic and Cationic Poly(amino acids) and Their Potential Applications in pH-Dependent Drug Delivery

Zoë Folchman-Wagner [1] **, Jennica Zaro** [2] **and Wei-Chiang Shen** [1,*]

[1] Department of Pharmaceutical Sciences, University of Southern California School of Pharmacy, 1985 Zonal Avenue, Los Angeles, CA 90089, USA; folchman@usc.edu

[2] Department of Pharmaceutical Sciences, West Coast University School of Pharmacy, 590 Vermont Ave, Los Angeles, CA 90004, USA; jzaro@westcoastuniversity.edu

* Correspondence: weishen@usc.edu

Abstract: Polyelectrolyte complexes (PECs) are self-assembling nano-sized constructs that offer several advantages over traditional nanoparticle carriers including controllable size, biodegradability, biocompatibility, and lack of toxicity, making them particularly appealing as tools for drug delivery. Here, we discuss potential application of PECs for drug delivery to the slightly acidic tumor microenvironment, a pH in the range of 6.5–7.0. Poly(L-glutamic acid) (E_n), poly(L-lysine) (K_n), and a copolymer composed of histidine-glutamic acid repeats (($HE)_n$) were studied for their ability to form PECs, which were analyzed for size, polydispersity, and pH sensitivity. PECs showed concentration dependent size variation at residue lengths of E_{51}/K_{55} and E_{135}/K_{127}, however, no complexes were observed when E_{22} or K_{21} were used, even in combination with the longer chains. $(HE)_{20}/K_{55}$ PECs could encapsulate daunomycin, were stable from pH 7.4–6.5, and dissociated completely between pH 6.5–6.0. Conversely, the $E_{51\text{-dauno}}/K_{55}$ PEC dissociated between pH 4.0 and 3.0. These values for pH-dependent particle dissociation are consistent with the pK_a's of the ionizable groups in each formulation and indicate that the specific pH-sensitivity of $(HE)_{20\text{-dauno}}/K_{55}$ PECs is mediated by incorporation of histidine. This response within a pH range that is physiologically relevant to the acidic tumors suggests a potential application of these PECs in pH-dependent drug delivery.

Keywords: polyelectrolyte complexes; drug delivery; pH-sensitive; histidine

1. Introduction

Polyelectrolyte complexes (PECs) are structures that form spontaneously upon combination of oppositely charged macromolecules in solution. The formation and physical characteristics of these complexes is driven by multiple factors including, but not limited to, molecular weight and ionic strength of each component, charge density, concentration, polymer chain rigidity, pH, and mixing intensity [1,2]. The type and concentration of salt in solution is also important as this can result in a neutralization of polymer charge [2,3]. The PECs are formed via an entropic process that has been previously described [4]. Briefly, the complex formation, while largely driven by electrostatics, also involves hydrogen bonding and Van der Waals interactions [1]. The mechanism can be broken into roughly three steps, the first of which is initial complex formation driven by electrostatic interactions, followed by formation of new bonds within this complex, and, lastly, the aggregation of multiple system complexes. The size of PECs is highly controllable, and can be affected by multiple factors including polymer molecular weight and concentration [4]. This property allows for uncomplicated production of PECs within a size range appropriate for drug delivery applications [5].

PECs have several advantages over alternative complexes or nanoparticles in that they have a highly controllable size, avoid toxic cross-linkers, and are biodegradable, biocompatible, and non-toxic [4,6]. Many iterations of PEC work exists in the literature [7–13], including extensive efforts using chitosan [6,14–19], and the complexes have been applied to fields that include drug delivery, gene delivery, and microencapsulation of both cells and tissues [1]. Due to their optimal physicochemical and biological properties, PECs are an ideal area of exploration for development and analysis of potential drug carriers. Owing to the highly controllable formation of PECs, it is of further interest to perform a closer examination of the self-assembly process and properties of PECs formed in a poly(amino-acid) solution. In addition to these advantages, PECs also present a unique opportunity in the potential for modular design enabled by the array of properties inherent to amino acids.

One possibility is to take advantage of the pH-dependent ionization in various amino acid side groups for the design of PECs whose assembly/disassembly properties are pH-sensitive. Previous studies in our lab have demonstrated that complexes between imidazole-modified poly-glutamic acid and polylysine, K_n, exhibited a response to environmental pH from 5 to 7 on complex formation [20]. Additionally, our lab has previously developed a pH-responsive peptide composed of repeats of glutamic acid and histidine, $(HE)_n$ [21]. The pH-responsiveness of this copolymer has been demonstrated at several repeat lengths including $(HE)_{15}$ [22], $(HE)_{10}$ [23], and $(HE)_{8-12}$ [24]. At physiologic pH of ~7.4, glutamic acid is negatively charged, while histidine remains unprotonated, giving $(HE)_n$ a net negative charge. As the pH is lowered, the imidazole group in histidine ($pK_a = 6.5$) becomes protonated, resulting in neutralization of the $(HE)_n$ copolymer. Thus, $(HE)_n$ may be used as a highly sensitive pH responsive switch, rapidly converting from charged to uncharged within the small pH window of 6.5–7. Here, we report the use of a longer version of the $(HE)_n$ copolymer than previously reported, with 20 repeats it is designated as $(HE)_{20}$.

In this study, we evaluated the combination of pH responsive $(HE)_n$ with K_n to create a pH-sensitive PEC, capable of forming at neutral pH due to electrostatic interaction of the negative glutamic acid and the positive lysine. At slightly acidic pH, both the histidine (cationic) and glutamic acid (anionic) residues in $(HE)_n$ are ionized, resulting in a net-neutral charge of the $(HE)_n$ copolymer and loss of electrostatic interaction with lysine. The physicochemical factors necessary for formation of PEC from K_n and E_n as well as K_n and the $(HE)_n$ copolymer, including the ultimate pH sensitivity of these PECs, were investigated. The chemotherapeutic drug daunomycin [25] was added to the PEC formed with K_n and $(HE)_n$ as proof of concept for utility as a drug delivery tool.

2. Materials and Methods

2.1. Poly(L-glutamic acid)/Poly(L-lysine) PECs

E_n and K_n were purchased from Alamanda Polymers (Huntsville, AL, USA). The degree of polymerization (DP_n), as determined by nuclear magnetic resonance spectroscopy, was for E_n, n = 22 (molecular weight (MW) = 3300) and n = 51 (MW = 7700) and for K_n, n = 21 (MW = 4400) and n = 55 (MW = 11,500). Aqueous solutions were prepared and filtered through 0.22 µm filters (Argos Technologies, Elgin, IL, USA). Larger molecular weight E_n (MW 15,000–50,000) and K_n (MW 15,000–30,000) with average DP_n of 135 and 127, respectively, were purchased from Sigma Aldrich (St. Louis, MO, USA).

E_n and K_n were mixed starting at E_n concentrations of 1 mg/mL, 0.5 mg/mL, 0.25 mg/mL, or 0.125 mg/mL with K_n at 1:1, or 1:2 molar charge in ddH$_2$O. PECs were formed by drop-wise addition of E_n into a stirred solution of K_n. E_n solution was added in 50 or 100 µL aliquots to 500 µL or 1 mL of K_n at 30 s intervals until the full volume of 500 µL or 1 mL was added. The resulting dispersion was stirred for an additional 10 min and then analyzed using dynamic light scattering (DLS) (Dynapro Plate Reader, Wyatt, Santa Barbara, CA, USA) to determine particle size.

Size readings were performed in quadruplicate, where data was shown as average size diameter reading over the four wells ± standard deviation (nm), and outliers were identified using Grubb's test with $\alpha = 0.05$. Studies on size and polydispersity of PECs were performed by incubating PEC

dispersions at either 25 °C or 4 °C for various periods of time followed by analysis of size variance and polydispersity index (PDI) using DLS.

2.2. Recombinant Expression of (HE)$_{20}$ Peptide

The pH-responsive (HE)$_{20}$ peptide was produced recombinantly as a glutathione S-transferase (GST)-(HE)$_n$ fusion protein containing a thrombin cutting site between the GST and (HE)$_n$ domains as previously described [23]. Briefly, plasmids containing the *GST-(HE)$_{20}$* gene were transformed into *Escherichia coli* expression strain BL21 and the recombinant protein was expressed as previously described [21,23,24]. The resultant bacterial pellets were resuspended in phosphate buffered saline (PBS) (pH 7.4) containing 0.25 mg/mL lysozyme. After incubation for 30 min on ice, phenylmethylsulfonyl fluoride (1 mM) and Triton X-100 (1%, *v/v*) were added to lyse the bacteria. The lysate was centrifuged (15,000× *g* for 30 min at 4 °C) and the supernatant was loaded onto a glutathione (GSH) agarose column pre-balanced with PBS. The GSH column was washed with 1% Triton X-100 in PBS followed by PBS, and then thrombin (Sigma) was loaded onto the agarose followed by incubation for 16 h at room-temperature. After thrombin cleavage, the (HE)$_{20}$ peptide was eluted with PBS and purified by nickel-nitriloacetic acid (Ni-NTA) agarose chromatography using 250 mM imidazole, pH 8.0 as the elution buffer [21]. (HE)$_{20}$ peptide was then dialyzed (molecular weight cut-off (MWCO) 3500 Da) against PBS to remove imidazole, and the purified (HE)$_{20}$ peptide was analyzed by SDS-PAGE with Coomassie blue staining to determine purity and confirm size. The final sequence of the peptide was (HE)$_{10}$-F-(HE)$_{10}$, abbreviated as "(HE)$_{20}$".

2.3. Formulation of PEC with Daunomycin, (HE)$_{20}$, and PLys$_{55}$

Daunomycin HCl was purchased from Cayman Chemical (Ann Arbor, MI, USA). PECs with daunomycin, (HE)$_{20}$, and K$_{55}$ were made by combining 1–0.125 mg/mL daunomycin with 1–0.125 mg/mL (HE)$_{20}$ at equal concentrations ((HE)$_{20\text{-dauno}}$). The (HE)$_{20\text{-dauno}}$ was then added dropwise to a stirred solution of K$_{55}$ at 1:1 (HE)$_{20\text{-dauno}}$:K$_{55}$ molar charge ratio. Resulting PECs were analyzed using DLS to determine particle size as well as fluorescence (excitation/emission of 480/590 nm) to determine daunomycin concentration and incorporation efficiency [26]. The encapsulation efficiency was determined by comparing the ratio of fluorescence intensity between free daunomycin to that of the (HE)$_{20\text{-dauno}}$/K$_{55}$ PEC.

2.4. Formulation of PEC with Daunomycin, (HE)$_{20\text{-dauno}}$, and K$_{55}$ in ZnCl$_2$·2NH$_4$Cl solution

ZnCl$_2$, NH$_4$Cl, and tricine were purchased from Sigma-Aldrich (St. Louis, MO, USA). ZnCl$_2$·2NH$_4$Cl was formed by mixing ZnCl$_2$ and NH$_4$Cl in a 1:2 molar ratio in ddH$_2$O, followed by dilution into a solution of 10 mg/mL tricine as chelator. The ZnCl$_2$·2NH$_4$Cl/tricine solution, at a 1:2 molar ratio to histidine in (HE)$_{20\text{-dauno}}$, was then used to dissolve K$_{55}$ (K$_{55\text{-Zn}}$). Then, 1 mg/mL daunomycin was added to an equivalent concentration of (HE)$_{20\text{-dauno}}$ dissolved in 10 mg/mL tricine and the pH increased to 8.0. The (HE)$_{20\text{-dauno}}$ solution was then added dropwise to a stirred solution of K$_{55\text{-Zn}}$ in tricine at a 1:1 (HE)$_{20\text{-dauno}}$:K$_{55}$ molar charge ratio. The resulting PECs were stirred for an additional 10 min and then analyzed by DLS.

2.5. Formulation of PEC with Daunomycin, E$_{51}$, and K$_{55}$ in ZnCl$_2$·2NH$_4$Cl solution

One milligram per milliliter daunomycin was added to 1 mg/mL E$_{51}$ solution (E$_{51\text{-dauno}}$) in ddH$_2$O prior to PEC formation. ZnCl$_2$ was prepared as described above and used to dissolve K$_{55}$ (K$_{55\text{-Zn}}$). The E$_{51\text{-dauno}}$ solution was then added dropwise to a stirred solution of K$_{55\text{-Zn}}$ in tricine at a 1:1 molar charge ratio. The resulting PECs were stirred for an additional 10 min, diluted into 10 mg/mL Tricine, and then analyzed by DLS.

2.6. pH Sensitivity of $E_{51\text{-}dauno}/K_{55\text{-}Zn}$ PEC and $(HE)_{20\text{-}dauno}/K_{55\text{-}Zn}$

To determine the pH sensitivity of the PEC formed from $E_{51\text{-}dauno}/K_{55\text{-}Zn}$ and $(HE)_{20\text{-}dauno}/K_{55\text{-}Zn}$, the PEC were formed in ddH$_2$O or 10 mg/mL tricine solutions. The $(HE)_{20\text{-}dauno}/K_{55\text{-}Zn}$ PEC were formed as described above in ddH$_2$O and then diluted into 10 mg/mL Tricine. The pH was adjusted using 1 N HCl, and monitored with an Orion PerpHecT ROSS combination pH Micro Electrode from ThermoFischer Scientific (Waltham, MA, USA). PEC were analyzed at intervals of 1 or 0.5 pH units by DLS; PEC degradation was determined by a DLS reading of 0.00 nm or an 'incomplete' reading.

3. Results and Discussion

3.1. PEC Formed from K_n and E_n

PEC showed a high degree of concentration and molecular weight dependence in ultimate hydrodynamic diameter. The PEC formed from E_{135}/K_{127} were significantly larger than the E_{51}/K_{55} and $2X\text{-}E_{51}/K_{55}$ at all concentrations tested (Figure 1). Further, as the concentration of K_n and E_n decreased, there was a corresponding decrease in the size of the PEC (Figure 1).
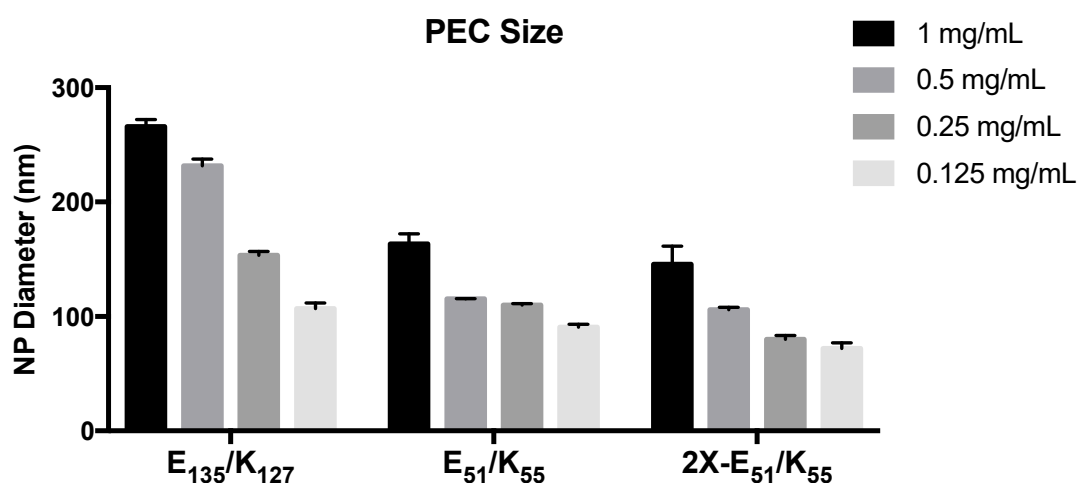

Figure 1. Size summary of poly(L-Lysine) (K_n) and poly(L-Glutamic Acid) (E_n) polyelectrolyte complexes (PECs). PECs were formulated at 1:1 or 1:2 molar charge ratios of E_n:K_n with the indicated degree of polymerization (DP$_n$) and beginning from an E_n concentration of 1 mg/mL. Decreasing the DP$_n$ of poly(L-Lysine) and poly(L-Glutamic Acid) from 127/135 to 55/51 resulted in a statistically significant decrease in diameter at all concentrations tested. All formulations demonstrated concentration dependence in diameter. Data shown are hydrodynamic diameter as determined by dynamic light scattering (DLS) and are the averages over 3–4 wells ± standard deviation. Results were analyzed by two-way ANOVA.

This trend was observed for the 1:1 charge ratio of E_{135}/K_{127}, the 1:1 charge ratio of E_{51}/K_{55}, and the 1:2 charge ratio of E_{51}/K_{55}. The concentration dependence of PECs was expected based on well-established models of aggregation by Debye models and Derjaguin, Landau, Verwey, and Overbeek Theory, as well as previous studies [27,28]. PEC formulated with a two-fold excess of positive charge ($2X\text{-}E_{51}/K_{55}$) were slightly smaller than those formed with an equal charge ratio. This size difference was significant at all concentrations except 0.5 mg/mL. When shorter poly amino-acid chains were used, K_{21} and E_{22}, no PEC formation could be seen at a 1:1 charge ratio for E_n concentration of 1 mg/mL or 2 mg/mL. When these shorter chains were combined with longer repeats, E_{51}/K_{21} and E_{22}/K_{55}, there remained no complex formation at a 1:1 charge ratio or 1:1 molar ratio. This result suggests that there is a critical limitation for PEC size using these poly amino-acids. As some of the driving factors for PEC formation include molecular weight, charge density, and hydrophobicity,

it is reasonable to suggest that the DP_n of 21 and 22 did not have sufficient charge density and/or hydrophobicity to nucleate the formation of PEC. The lack of PEC formation even when paired with a long poly amino-acid further supports this claim that there is a bottom limit to PEC formation when working with these short chain amino-acids. The details of this process are as yet unclear, as the process of PEC formation is multi-step. It is well established that increasing concentration of poly-electrolytes in solution decreases the Debye length of the system, resulting in a reduction in electrostatic repulsion [29,30]. It is, therefore, possible that the short chain length of K_{21} and E_{22} did not have enough charge density to decrease the Debye length, resulting in high electrostatic repulsion.

The E_{51}/K_{55} and 2X-E_{51}/K55 were analyzed for size and polydispersity at 25 °C and 4 °C (Figures 2 and 3) at various concentrations from 1 to 0.125 mg/mL E_{51}.
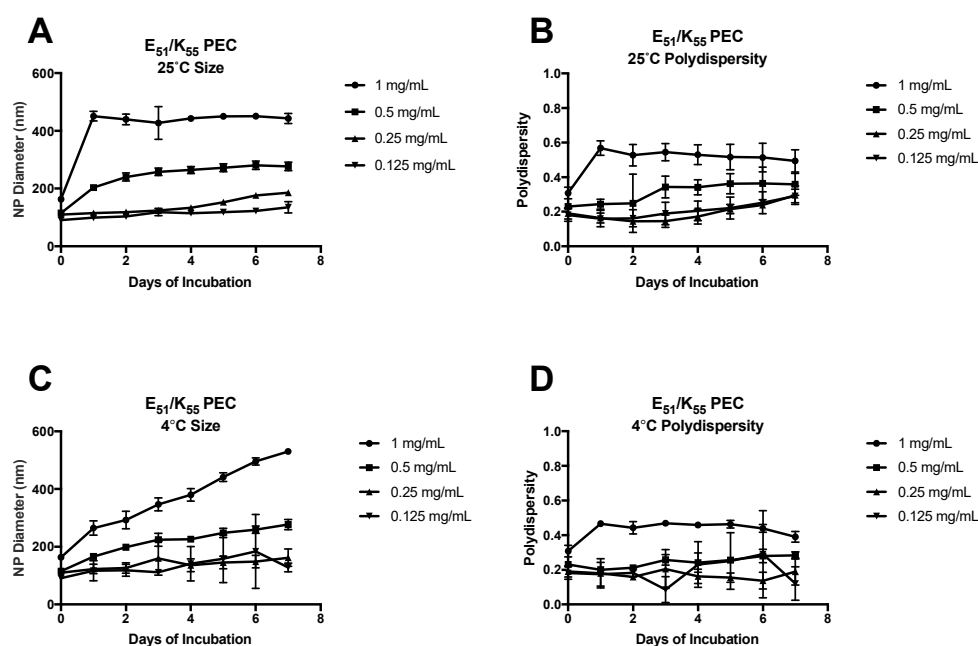

Figure 2. Stability of E_{51}/K_{55} PEC formed from 1:1 charge ratio at 25 °C and 4 °C. Panels (**A**,**B**) show the size and polydispersity, respectively, of PEC formed from E_{51} and K_{55} at a 1:1 charge ratio at 25 °C over 7 days. At 1 mg/mL and 0.5 mg/mL there was an increase in size and polydispersity after 24–72 h of incubation, followed by plateau. The 0.25 and 0.125 mg/mL formulations showed little change in diameter over 7 days and a slight increase in polydispersity; Panels (**C**,**D**) show the size and polydispersity, respectively, of PEC formed from E_{51} and K_{55} at a 1:1 charge ratio at 4 °C over 7 days. No plateau was reached in diameter for the 1 mg/mL or 0.5 mg/mL formulations, while the 0.25 and 0.125 mg/mL formulations showed little change. The polydispersity showed an increase after 24 h in the 1 mg/mL formulation, followed by plateau, while the lower concentrations remained nearly constant with minor fluctuations. Data were obtained by DLS, and are displayed as averages over 3–4 wells ± standard deviation.

At the high end of the concentration range, with E_n concentration of 1 mg/mL, the E_{51}/K_{55} PEC showed a dramatic increase in diameter after 24 h of 25 °C incubation, nearly doubling in size, and were then constant for 7 days (Figure 2A). The polydispersity of these PEC showed the same initial increase, then proceeded with a downward trend up to the last time-point (Figure 2B). When stored at 4 °C, the E_{51}/K_{55} PEC at 1 mg/mL E_{51} had a gradual and sustained increase in size up to the last time point, with no clear plateau reached (Figure 2C). The polydispersity of the 1 mg/mL formulation at 4 °C increased after 24 h and was most stable for the following 6 days (Figure 2D). A similar trend was seen in the PEC formed at an E_{51} concentration of 0.5 mg/mL, however, the size increase in both storage temperatures was more gradual, and no clear size plateau was reached at 4 °C. The polydispersity at 0.5 mg/mL, when stored at 25 °C, showed no change until day 3, where there was an

increase from ~0.2 to ~0.35, followed by stabilization of the reading for the remaining 4 days. PEC formed from 0.25 and 0.125 mg/mL were mostly constant in size at both storage conditions. Under a 25°C incubation, the PEC were stable in size for approximately 5 days before increasing slightly. At 4 °C, the PEC remained at a stable size for the full 7 days. The polydispersity was more varied for these lower concentration PECs. The 0.5 mg/mL E_{51} displayed a trend similar to 1 mg/mL of increase followed by plateau, however, the 0.25 and 0.125 mg/mL E_{51} PEC maintained a fairly constant polydispersity but began to show a slight increase after 4 days of incubation at 25 °C. At 4 °C the polydispersity remained constant, however, there was noticeably higher, although not statistically significant, deviation between days.

Similar trends in stability were observed for the PEC formulated with a 2-fold molar charge excess of K_{55} over E_{51} (Figure 3).
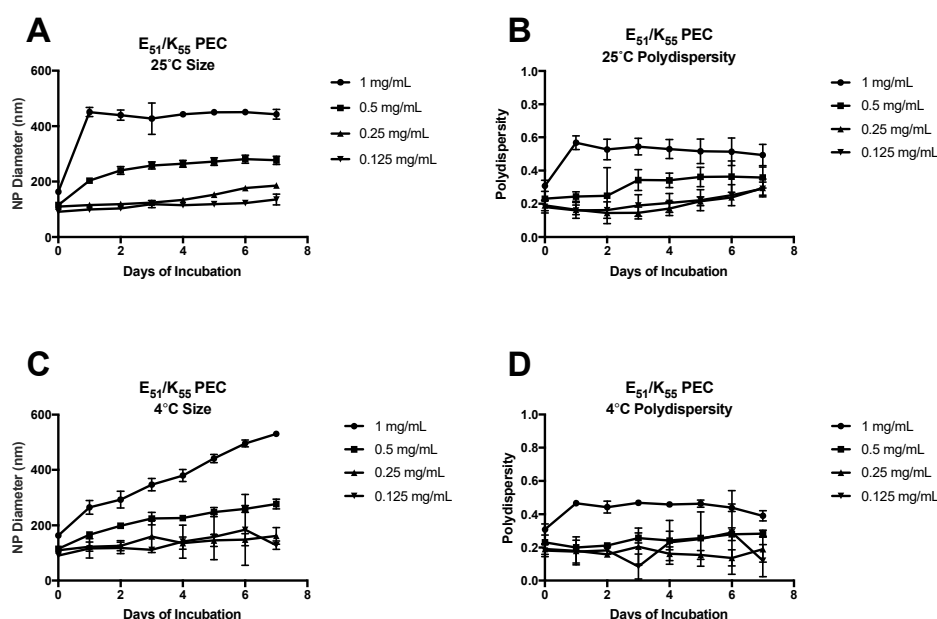

Figure 3. Stability of E_{51}/K_{55} PEC formed from 1:2 charge ratio at 25 °C and 4 °C. Panels (**A,B**) show the size and polydispersity, respectively, of PEC formed from E_{51} and K_{55} at a 2:1 charge ratio at 25 °C over 7 days. At 1 mg/mL and 0.5 mg/mL there was an increase in size after 24 h of incubation, followed by plateau. There was little change in polydispersity. The 0.25 and 0.125 mg/mL formulations showed little change in diameter or polydispersity over 7 days; Panels (**C,D**) show the size and polydispersity, respectively, of PEC formed from E_{51} and K_{55} at a 2:1 charge ratio at 4 °C over 7 days. All formulations except 0.125 mg/mL showed a gradual increase in size over 7 days. The 0.125 mg/mL formulation showed no significant change in diameter during the 7 day incubation. The 1 and 0.5 mg/mL formulations increased in polydispersity for three days before reaching a plateau, while the 0.25 and 0.125 mg/mL formulations remained stable until day 7, where there was an increase in the polydispersity. Data were obtained by DLS, and are displayed as averages over 3–4 wells $\pm$ standard deviation.

With the higher concentration of poly amino-acid solutions (1 mg/mL and 0.5 mg/mL), the complexes stored at 25 °C increased sharply in size after 24 h, and then remained constant for the remaining 7 days (Figure 3A). The polydispersity of these complexes remained consistent for 7 days of 25 °C incubation (Figure 3B). Conversely, for the PEC stored at 4 °C, the complex size increased slowly up to day 3, and remained relatively constant after that (Figure 3C). The polydispersity of the 4 °C PEC was inconsistent with that at 25 °C, showing an increase for 3 days, followed by plateau (Figure 3D). The 0.5 mg/mL E_{51} concentration PEC demonstrated a similar 24 h increase at 25 °C followed by plateau, while the 4 °C PEC increased in size steadily for the 7 days of the study. The polydispersity of the 25 °C formulation remained fairly constant throughout the 7 days, while the polydispersity of

the 4 °C formulation increased slowly for 3 days before leveling off. The 0.25 mg/mL concentration formulation showed a very gradual increase in diameter and reached a plateau after approximately 3 days, while the 4 °C formulation continued to show small daily size increases with no plateau. The polydispersity for both formulations was relatively constant, with a sharp increase after 7 days at 4 °C. Lastly, the most dilute of the formulations, 0.125 mg/mL, displayed a fairly constant size for all 7 days of the experiment. Similarly, the 4 °C formulation did not change in size in the dispersion at ~80 nm until day 7. There was no significant change in polydispersity during the 25 °C incubation, while the 4 °C incubation remained constant until day 7, where it increased from ~0.3 to ~0.5.

The plateau reached in almost all cases except the most dilute formulation suggests that there is a most stable form of the E_n/K_n PEC. The last step in PEC formation, as outlined in the introduction, is aggregation of multiple complexes formed by electrostatic interactions [1,4,30]. This is likely a dynamic process that continues until an equilibrium is reached [30]. The lack of plateau in the 4 °C storage is likely due to a decrease in the thermodynamic potential of the system, thus, increasing the time to equilibrium. The PEC formulated with a 2-fold molar excess of K_n should have a large positive surface charge, thus, providing electrostatic stability to the system by repulsion between neighboring complexes. In most cases, there is a decrease in time for equilibrium plateau to be reached, which tended to occur after 24 h of incubation.

3.2. Formulation of PEC with Daunomycin, $(HE)_{20}$, and K_{55}

Initial formulation of PEC with E_n/K_n was crucial in establishing both the technique for and limitations of the complex formation. Preliminary experiments utilizing the $(HE)_{10}$ peptide mixed with K_{21} and E_{22} did not form complexes, as expected based on results with E_{22} and K_{21}. Therefore, the number of HE-repeats was increased to n = 20 $((HE)_{20})$. In these complexes, no PEC formation was possible without the addition of daunomycin. Once daunomycin was added into the formulation, the homogeneity of the resulting PEC was dependent on whether daunomycin was added to the polyanion $((HE)_{20})$ or polycation (K_{55}) phase (Figure 4).
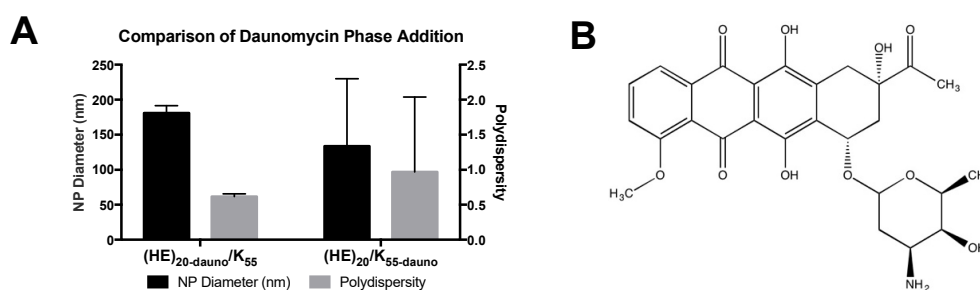

Figure 4. Comparison of daunomycin phase addition. (**A**) In two separate experiments daunomycin was dissolved in the histidine and glutamic acid peptide $((HE)_{20})$ solution $((HE)_{20\text{-dauno}})$ prior to PEC formation or in the K_{55} solution $(K_{55\text{-dauno}})$. The PEC formed from $(HE)_{20\text{-dauno}}$ and K_{55} were ~180 ± 10 nm in diameter with a polydispersity index (PDI) of 0.6 ± 0.04. Conversely the PEC formed from $(HE)_{20}$ and $K_{55\text{-dauno}}$ were ~130 ± 96 nm in diameter with a PDI of 0.96 ± 1.0. Data shown are averages of 4 wells ± standard deviation; (**B**) Structure of encapsulated daunomycin.

When daunomycin was combined with $(HE)_{20}$ prior to PEC formation $((HE)_{20\text{-dauno}}/K_{55})$, the resulting complexes were approximately 180 nm with a PDI of 0.60. There was, additionally, low deviation between the samples tested. Conversely, when daunomycin was added to the polycation prior to PEC formation $((HE)_{20}/K_{55\text{-dauno}})$, the resulting complexes were ~133 nm in diameter with a PDI of nearly 1. Additionally, there was large variation between samples for the PEC formed from $(HE)_{20}/K_{55\text{-dauno}}$, with standard deviation of ~100 nm for PEC diameter and ~1.0 for PDI (Figure 4).

These results suggest that the incorporation of daunomycin into the PEC is driven by both electrostatic and hydrophobic interactions. At pH values above the pK_a of histidine (6.5), the $(HE)_{20}$ copolymer will

have a net negative charge and is, therefore, capable of electrostatic interaction between the positively charged daunomycin (pK_a 8.4 [31]) and the gamma-carboxyl group of glutamic acid in $(HE)_{20}$. Further interaction may be possible due to hydrophobic interactions between the hydrophobic daunomycin (logP 1.8 [32]) and the histidine residues in the $(HE)_{20}$ copolymer. The polycationic K_{55} lacks the potential for electrostatic interaction with daunomycin, and the higher charge density of the lysines would likely repel interactions with the drug. The lack of discrete PEC formation upon addition of daunomycin to the polycation K_{55} phase supports the probability that the driving force for encapsulation of daunomycin in the PECs is electrostatic and hydrophobic interactions between daunomycin and $(HE)_{20}$, which form prior to the addition of the polyanion phase and, thus, result in drug incorporation once the $(HE)_{20}/K_{55}$ PECs are formed. Based on the heterogeneity of the $(HE)_{20}/K_{55\text{-dauno}}$ PEC, the daunomycin was exclusively added to the polyanion phase, $(HE)_{20}$, in all further formulations.

PEC formed from $(HE)_{20\text{-dauno}}/K_{55}$ showed a decrease in the fluorescent signal of daunomycin (Figure 5) at all concentrations tested. The fluorescence quenching observed in Figure 5 was attributed to encapsulation of daunomycin within the PEC, thus dampening the fluorescent signal [33]. The fluorescence intensity of free daunomycin was compared to the fluorescent signal of the $(HE)_{20\text{-dauno}}/K_{55}$ PEC, and the decrease in signal was taken as proportional to encapsulation efficiency. The loading amount (wt %) of daunomycin in PEC solutions with concentrations of 1–0.125 mg/mL polyanion and an equal molar charge of polycation, was 36% at all formulations. The encapsulation efficiency ranged from 58% to 85% (Table 1).

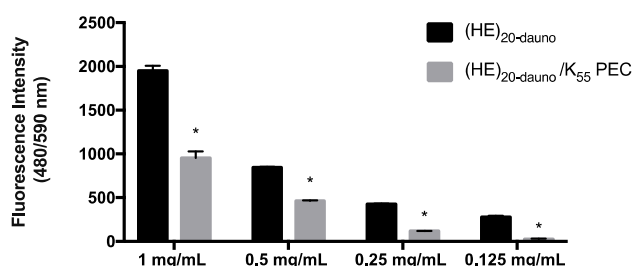**Figure 5.** Fluorescence quenching of daunomycin in $(HE)_{20\text{-dauno}}/K_{55}$ PEC. Fluorescence measurements were taken of the $(HE)_{20\text{-dauno}}$ solution alone and the $(HE)_{20\text{-dauno}}/K_{55}$ PEC. There is a significant decrease in fluorescence signal from daunomycin at all concentrations of PEC. The data shown are averages over 4 wells $\pm$ standard deviation. Results were analyzed by the Student's *t*-test, with $p < 0.001$ indicated (*).

Table 1. Encapsulation efficiency and loading content of daunomycin in $(HE)_{20\text{-dauno}}/K_{55}$ PEC. Fluorescence measurements were taken of the daunomycin solution alone and the $(HE)_{20\text{-dauno}}/K_{55}$ PEC. The ratio between free drug and drug encapsulated within the PEC was used to determine the encapsulation efficiency and loading content.

Daunomycin Concentration (mg/mL)	Encapsulation Efficiency, %	Loading Content, wt %
1	68%	25%
0.5	58%	21%
0.25	74%	27%
0.125	85%	31%

The $(HE)_{20\text{-dauno}}/K_{55}$ complexes also demonstrated a concentration dependent size decrease, with average diameter and polydispersity decreasing as the concentration prior to formulation decreased (Figure 6). These PEC further demonstrate the degree of control available for the ultimate size of the complexes formed.
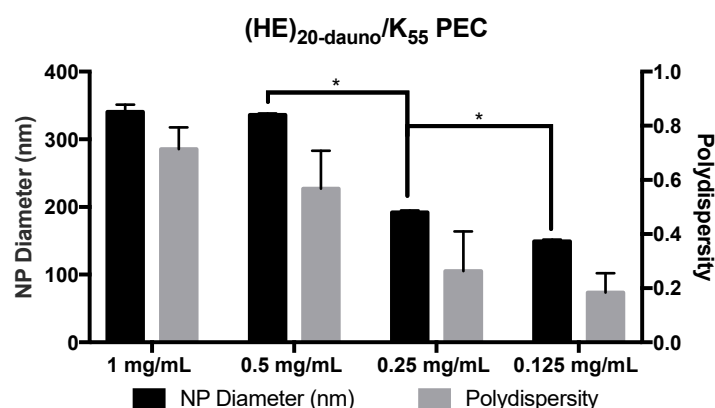
Figure 6. PEC formulated from $(HE)_{20\text{-dauno}}$ and K_{55} PEC formulated from $(HE)_{20\text{-dauno}}/K_{55}$ demonstrated significant concentration dependence in size at concentrations below 1 mg/mL. Polydispersity of the PEC decreased along with the size, and was statistically significant at concentrations below 1 mg/mL. Data shown are averages of four wells $\pm$ standard deviation. Results were analyzed by two-way ANOVA with $p < 0.05$ indicated (*).

3.3. Formulation of PEC with Daunomycin, $(HE)_{20}$, and K_{55} in $ZnCl_2 \cdot 2NH_4Cl$ Solution

While the PEC did form between $(HE)_{20\text{-dauno}}$ and K_{55}, the resulting formulations were of varying size with high polydispersity (Figure 6). To mitigate this problem, studies were performed with the addition of zinc to stabilize the PEC through metal ion coordination [34–36], thus serving as a stabilizer for the PEC. Histidine is able to coordinate divalent metal ions, including zinc, with high affinity through two to six histidine residues [37]. Additionally, there is evidence for doxorubicin interaction with zinc [38], specifically through the two keto-phenolate substituents [39], which are maintained in daunomycin. The ability of zinc to interact strongly with not only histidine but carbonyl residues is well documented [39–41] and, thus, provides the chemical basis for interactions between the zinc ions, the $(HE)_{20}$ copolymer, and encapsulated daunomycin. Therefore, zinc was added to the polycation phase to increase the number of interactions between the $(HE)_{20\text{-dauno}}$ and K_{55} to include electrostatic, hydrophobic, and metal ion coordination. Zinc was added to solution in the form of zinc ammonium chloride and dissolved in 10 mg/mL tricine, which was used as a chelator. The zinc ammonium chloride and tricine solution was used to dissolve K_{55}, followed by PEC formation as described above. These complexes were significantly smaller in size and had far lower polydispersity (Figure 7) illustrating the effect of the zinc ions in providing additional interaction potential between the $(HE)_{20\text{-dauno}}$ and K_{55}. The $(HE)_{20\text{-dauno}}/K_{55\text{-Zn}}$ complexes continued to exhibit a concentration dependent size (Figure 7).

3.4. pH Sensitivity of $E_{51\text{-dauno}}/K_{55\text{-Zn}}$ PEC and $(HE)_{20\text{-dauno}}/K_{55\text{-Zn}}$

The $(HE)_{20\text{-dauno}}/K_{55\text{-Zn}}$ PEC exhibited a high degree of pH sensitivity, dissociating completely at a pH between 6.0 and 6.5 (Figure 8). The complexes were stable in size at pH values of 7.4, 7.0 and 6.5, with little variation in diameter or increase in deviation. The PEC formulated with $E_{51\text{-dauno}}/K_{55\text{-Zn}}$ showed a high degree of variation in size from pH 7.4–4.0, and dissociated completely between pH 3.0 and 4.0 (Figure 8). These results indicate that the pH dependence of the $(HE)_{20\text{-dauno}}/K_{55\text{-Zn}}$ PEC is specifically mediated by the histidine present in $(HE)_{20}$. $(HE)_{20}$, as described above, has a pK_a of 6.5 for the imidazole group in histidine. At pH 6.5, there will be a 1:1 ratio of ionized to unionized histidine residues. The PEC formation is dependent on charge interaction between the negative glutamic acid of $(HE)_{20}$ and the positive lysine of K_{55}. When histidine in $(HE)_{20}$ begins to protonate, the overall charge of the $(HE)_{20}$ copolymer is lost, resulting in loss of the electrostatic interactions that held together the PEC. This result was also seen in the $E_{51\text{-dauno}}/K_{55\text{-Zn}}$, which dissociates at a pH of 3.0, a value below the pK_a of the gamma-carboxyl group of glutamic acid in E_{51}. The loss of charge on the $(HE)_{20}$ copolymer at pH 6.0–6.5 will additionally result in loss of the electrostatic interactions present in the $(HE)_{20}$-daunomycin

interaction discussed previously. Therefore, it is likely that loss of the PEC will also result in a release of daunomycin from interaction with $(HE)_{20}$ and the accumulation of free drug in solution.
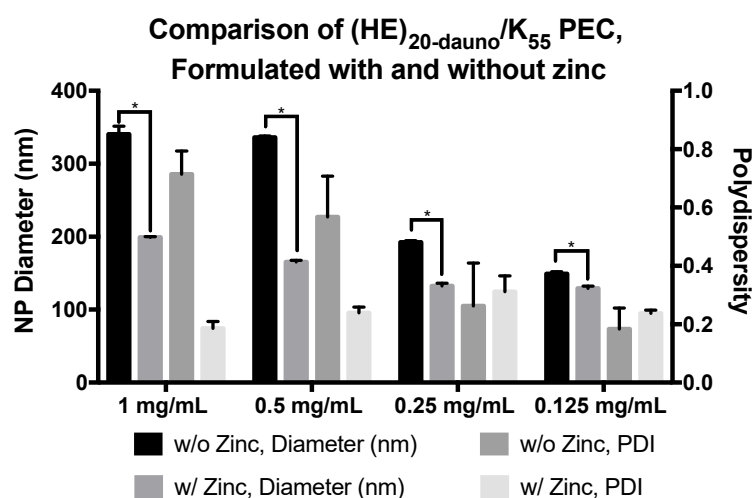

Figure 7. Comparison of PEC formulated from $(HE)_{20-dauno}$ and K_{55} with and without zinc. PEC formulated from $(HE)_{20-dauno}/K_{55}$ with zinc were significantly smaller at all concentrations tested than those without zinc. There was a corresponding decrease in polydispersity that was most apparent at the 1 mg/mL and 0.5 mg/mL formulations, however, it was not statistically significant. Data shown are averages of four wells ± standard deviation. Results were analyzed by two-way ANOVA with $p < 0.0001$ indicated (*).
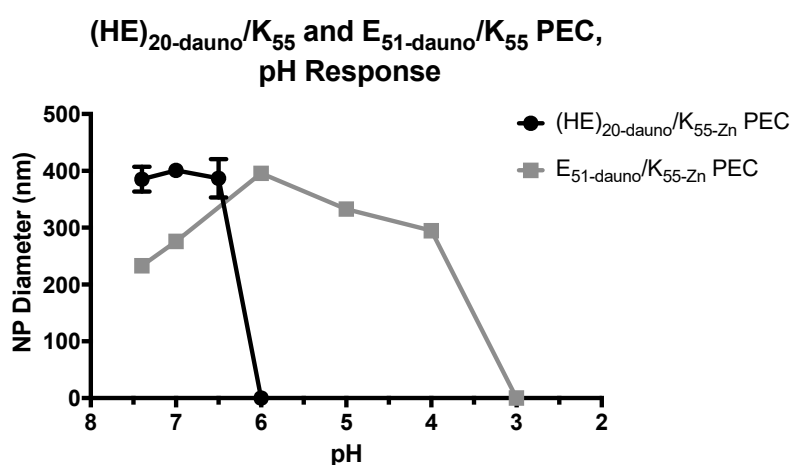

Figure 8. pH dependence of $(HE)_{20-dauno}/K_{55-Zn}$ PEC and $E_{51-dauno}/K_{55-Zn}$ PEC formulated with $(HE)_{20}$ demonstrate a high degree of pH sensitivity, with complete complex degradation between pH 6.5–6.0. Complex size stayed constant until pH 6.0. PEC formulated from E_{51} and K_{55} showed high variability in complex size over the pH range tested and did not degrade until between pH 4.0–3.0. These data show that the pH sensitivity exhibited by the $(HE)_{20-dauno}/K_{55-Zn}$ PEC is specifically mediated by the histidine present in $(HE)_{20}$. Data shown are averages of 3–4 wells ± standard deviation.

4. Summary

This paper outlines the formulation of polyelectrolyte complexes composed of cationic and anionic poly(amino acids). Formulations of PEC with poly(glutamic-acid) and poly(lysine) showed concentration dependent size variation at lengths of E_{51}/K_{55} and E_{135}/K_{137}, however, no PECs were observed when E_{22} or K_{21} were used, even in combination with longer chain-length E_{51} or K_{55} at charge ratios of 1:1, or 1:2. This result suggests a size limitation in PEC formation with these poly(amino

acids). While the specific formation process with these poly(amino acids) has yet to be elucidated, it is possible that the short chain length of K_{21} and E_{22} did not have enough charge density to decrease the Debye length, resulting in high electrostatic repulsion and a lack of successful PEC. Complexes formed with E_{51}/K_{55} and a two-fold positive charge excess, $2X\text{-}E_{51}/K_{55}$, were shown to exhibit a fairly rapid increase in size after 24 h followed by plateau. The change in size was most dramatic at the highest concentrations studied (1 mg/mL and 0.5 mg/mL), with a much smaller size increase at lower concentrations.

To investigate the potential pH sensitivity of these PECs, a $(HE)_{20}$ copolymer composed of repeats of histidine and poly(glutamic acid) was used in place of E_n for complex formation. Histidine has previously shown potential as a tool for pH-sensitive drug delivery [42–47] and the $(HE)_{20}$ copolymer specifically has been shown to enable pH-dependent internalization of cell penetrating peptides [21,23], thus making it a promising candidate for formation of pH-sensitive PECs. The $(HE)_{20}$ copolymer was mixed with K_{55} at 1:1 molar charge ratios and, in the presence of zinc, was able to encapsulate the anticancer drug daunomycin. These $(HE)_{20\text{-dauno}}/K_{55\text{-Zn}}$ PEC showed a high degree of pH responsiveness, maintaining a ~400 nm diameter at pH values of 7.4–6.5, and dissociating completely between pH 6.5 and 6.0. In contrast, PEC formed with $E_{51\text{-dauno}}/K_{55\text{-Zn}}$ did not dissociate until between pH 4.0 and 3.0. This large difference in pH response is likely mediated specifically by the incorporation of histidine in the $(HE)_{20}$ copolymer. $(HE)_{20}$ will have a net negative charge at pH values above ~6.5, however, histidine has a pK_a of 6.5 and so at a pH of 6.5 will be 50% ionized. This ionization partially neutralizes the negative charge of $(HE)_{20}$, and as the copolymer loses its net negative charge, the electrostatic interactions with K_n driving the PEC formation are lost, and the particle dissociates. The $E_{51\text{-dauno}}/K_{55\text{-Zn}}$ particles, lacking histidine, do not dissociate until a pH between pH 4.0 and 3.0, which is close to the pK_a of poly(glutamic acid). At pH 3.0 the poly(glutamic acid) residues start to become protonated, thus losing the charge-based interaction with K_n and falling apart.

The use of pH-responsive platforms for drug delivery has garnered increased attention due to the fact that solid tumors possess a slightly acidic environment (pH 6.5–7) compared to that of healthy physiologic fluid (pH 7.4) [48–53]. This enables the use of stimulus-sensitive carriers, such as the $(HE)_{20\text{-dauno}}/K_{55\text{-Zn}}$ PEC, that respond to the change in pH found in the tumor microenvironment by dissociation of the carrier complex. Further studies in the release profiles of these pH-responsive PECs may illustrate the use of these complexes in enabling site-specific drug release directly to the tumor microenvironment, ultimately resulting in higher specificity of drug action, lower side-effects, and reduced dosage. The $(HE)_{20\text{-dauno}}/K_{55\text{-Zn}}$ PEC demonstrate a controllable size and pH response and offer a highly modular platform from which to continue further studies into the use of this technology for pH-dependent drug delivery to the tumor microenvironment.

5. Conclusions

This paper outlines the production of polyelectrolyte complex nanoparticles formulated from poly(L-glutamic acid) and poly(L-lysine) at low concentrations from 1 to 0.125 mg/mL. The complexes formed are highly controllable in size, and a critical length limitation of >~50 repeats was noted for successful complex formation. The addition of histidine to these complexes, in the form of the copolymer $(HE)_{20}$, resulted in polyelectrolyte nanoparticles that retained a high dependence on concentration for ultimate size. Additionally, the $(HE)_{20}/K_{55}$ nanoparticles, with encapsulated daunomycin and zinc, were highly pH-responsive, degrading completely between pH 6.5–6.0, demonstrating the effectiveness of histidine in conferring pH-sensitivity.

Author Contributions: Z.F.-W., J.Z. and W.-C.S. conceived and designed the experiments; Z.F.-W. performed the experiments; Z.F.-W., J.Z. and W.-C.S. analyzed the data; Z.F.-W. wrote the paper; Z.F.-W., J.Z. and W.-C.S. edited the paper.

Conflicts of Interest: The authors declare no conflict of interest.

References

1. Hartig, S.M.; Greene, R.R.; Dikov, M.M.; Prokop, A.; Davidson, J.M. Multifunctional nanoparticulate polyelectrolyte complexes. *Pharm. Res.* **2007**, *24*, 2353–2369. [CrossRef] [PubMed]

2. Langevin, D. Complexation of oppositely charged polyelectrolytes and surfactants in aqueous solutions. A review. *Adv. Colloid Interface Sci.* **2009**, *147–148*, 170–177. [CrossRef] [PubMed]

3. Domard, A.; Rinaudo, M. Polyelectrolyte Complexes. Interaction of Poly(L-lysine)-Poly(L-glutamic acid) in Dilute Aqueous Solution. *Macromolecules* **1980**, *13*, 898–904. [CrossRef]

4. Kulkarni, A.D.; Vanjari, Y.H.; Sancheti, K.H.; Patel, H.M.; Belgamwar, V.S.; Surana, S.J.; Pardeshi, C.V. Polyelectrolyte complexes: Mechanisms, critical experimental aspects, and applications. *Artif. Cells Nanomed. Biotechnol.* **2016**, 1–11. [CrossRef] [PubMed]

5. Ma, N.; Ma, C.; Li, C.; Wang, T.; Tang, Y.; Wang, H.; Moul, X.; Chen, Z.; Hel, N. Influence of nanoparticle shape, size, and surface functionalization on cellular uptake. *J. Nanosci. Nanotechnol.* **2013**, *13*, 6485–6498. [CrossRef] [PubMed]

6. Rasente, R.Y.; Imperiale, J.C.; Lazaro-Martinez, J.M.; Gualco, L.; Oberkersch, R.; Sosnik, A.; Calabrese, G.C. Dermatan sulfate/chitosan polyelectrolyte complex with potential application in the treatment and diagnosis of vascular disease. *Carbohydr. Polym.* **2016**, *144*, 362–370. [CrossRef] [PubMed]

7. Dai, W.G.; Dong, L.C. Characterization of physiochemical and biological properties of an insulin/lauryl sulfate complex formed by hydrophobic ion pairing. *Int. J. Pharm.* **2007**, *336*, 58–66. [CrossRef] [PubMed]

8. Yang, L.; Cui, F.; Shi, K.; Cun, D.; Wang, R. Design of high payload PLGA nanoparticles containing melittin/sodium dodecyl sulfate complex by the hydrophobic ion-pairing technique. *Drug Dev. Ind. Pharm.* **2009**, *35*, 959–968. [CrossRef] [PubMed]

9. Sun, S.; Liang, N.; Kawashima, Y.; Xia, D.; Cui, F. Hydrophobic ion pairing of an insulin-sodium deoxycholate complex for oral delivery of insulin. *Int. J. Nanomed.* **2011**, *6*, 3049–3056. [CrossRef]

10. Muller, M.; Reihs, T.; Ouyang, W. Needlelike and spherical polyelectrolyte complex nanoparticles of poly(L-lysine) and copolymers of maleic acid. *Langmuir ACS J. Surf. Colloids* **2005**, *21*, 465–469. [CrossRef] [PubMed]

11. Reihs, T.; Muller, M.; Lunkwitz, K. Preparation and adsorption of refined polyelectrolyte complex nanoparticles. *J. Colloid Interface Sci.* **2004**, *271*, 69–79. [CrossRef] [PubMed]

12. Akagi, T.; Kaneko, T.; Kida, T.; Akashi, M. Preparation and characterization of biodegradable nanoparticles based on poly(gamma-glutamic acid) with L-phenylalanine as a protein carrier. *J. Control. Release Off. J. Control. Release Soc.* **2005**, *108*, 226–236. [CrossRef] [PubMed]

13. Akagi, T.; Watanabe, K.; Kim, H.; Akashi, M. Stabilization of polyion complex nanoparticles composed of poly(amino acid) using hydrophobic interactions. *Langmuir* **2010**, *26*, 2406–2413. [CrossRef] [PubMed]

14. Wu, Q.X.; Lin, D.Q.; Yao, S.J. Design of chitosan and its water soluble derivatives-based drug carriers with polyelectrolyte complexes. *Mar. Drugs* **2014**, *12*, 6236–6253. [CrossRef] [PubMed]

15. Cerchiara, T.; Abruzzo, A.; Parolin, C.; Vitali, B.; Bigucci, F.; Gallucci, M.C.; Nicoletta, F.P.; Luppi, B. Microparticles based on chitosan/carboxymethylcellulose polyelectrolyte complexes for colon delivery of vancomycin. *Carbohydr. Polym.* **2016**, *143*, 124–130. [CrossRef] [PubMed]

16. Mocchiutti, P.; Schnell, C.N.; Rossi, G.D.; Peresin, M.S.; Zanuttini, M.A.; Galvan, M.V. Cationic and anionic polyelectrolyte complexes of xylan and chitosan. Interaction with lignocellulosic surfaces. *Carbohydr. Polym.* **2016**, *150*, 89–98. [CrossRef] [PubMed]

17. Luo, Y.; Wang, Q. Recent development of chitosan-based polyelectrolyte complexes with natural polysaccharides for drug delivery. *Int. J. Biol. Macromol.* **2014**, *64*, 353–367. [CrossRef] [PubMed]

18. Hamman, J.H. Chitosan Based Polyelectrolyte Complexes as Potential Carrier Materials in Drug Delivery Systems. *Mar. Drugs* **2010**, *8*, 1305–1322. [CrossRef] [PubMed]

19. Delair, T. Colloidal polyelectrolyte complexes of chitosan and dextran sulfate towards versatile nanocarriers of bioactive molecules. *Eur. J. Pharm. Biopharm* **2011**, *78*, 10–18. [CrossRef] [PubMed]

20. Shen, W.C. Acid-Sensitive Dissociation between Poly(Lysine) and Histamine-Modified Poly(Glutamate) as a Model for Drug-Releasing from Carriers in Endosomes. *Biochim. Biophys. Acta* **1990**, *1034*, 122–124. [CrossRef]

21. Zaro, J.L.; Fei, L.; Shen, W.C. Recombinant peptide constructs for targeted cell penetrating peptide-mediated delivery. *J. Control. Release* **2012**, *158*, 357–361. [CrossRef] [PubMed]

22. Yeh, T.-H.; Chen, Y.-R.; Chen, S.-Y.; Shen, W.-C.; Ann, D.K.; Zaro, J.L.; Shen, L.-J. Selective intracellular delivery of recombinant arginine deiminase (ADI) using pH-sensitive cell penetrating peptides to overcome ADI resistance in hypoxic breast cancer cells. *Mol. Pharm.* **2015**, *13*, 262–271. [CrossRef] [PubMed]

23. Fei, L.; Yap, L.P.; Conti, P.S.; Shen, W.C.; Zaro, J.L. Tumor targeting of a cell penetrating peptide by fusing with a pH-sensitive histidine-glutamate co-oligopeptide. *Biomaterials* **2014**, *35*, 4082–4087. [CrossRef] [PubMed]

24. Sun, C.M.; Shen, W.C.; Tu, J.S.; Zaro, J.L. Interaction between Cell-Penetrating Peptides and Acid-Sensitive Anionic Oligopeptides as a Model for the Design of Targeted Drug Carriers. *Mol. pharm.* **2014**, *11*, 1583–1590. [CrossRef] [PubMed]

25. Bains, O.S.; Szeitz, A.; Lubieniecka, J.M.; Cragg, G.E.; Grigliatti, T.A.; Riggs, K.W.; Reid, R.E. A Correlation between Cytotoxicity and Reductase-Mediated Metabolism in Cell Lines Treated with Doxorubicin and Daunorubicin. *J. Pharm. Exp. Ther.* **2013**, *347*, 375–387. [CrossRef] [PubMed]

26. Htun, M.T. Photophysical study on daunorubicin by fluuorescence spectroscopy. *J. Lumin.* **2009**, *129*, 344–348. [CrossRef]

27. Starchenko, V.; Muller, M.; Lebovka, N. Sizing of PDADMAC/PSS complex aggregates by polyelectrolyte and salt concentration and PSS molecular weight. *J. Phys. Chem. B* **2012**, *116*, 14961–14967. [CrossRef] [PubMed]

28. Buchhammer, H.M.; Mende, M.; Oelmann, M. Formation of mono-sized polyelectrolyte complex dispersions: Effects of polymer structure, concentration and mixing conditions. *Colloid Surf. A* **2003**, *218*, 151–159. [CrossRef]

29. Wandrey, C.; Hunkeler, D.; Wendler, U.; Jaeger, W. Counterion activity of highly charged strong polyelectrolytes. *Macromolecules* **2000**, *33*, 7136–7143. [CrossRef]

30. Muller, M.; Kessler, B.; Frohlich, J.; Poeschla, S.; Torger, B. Polyelectrolyte Complex Nanoparticles of Poly(ethyleneimine) and Poly(acrylic acid): Preparation and Applications. *Polymers* **2011**, *3*, 762–778. [CrossRef]

31. Gallois, L.; Fiallo, M.; Garnier-Suillerot, A. Comparison of the interaction of doxorubicin, daunorubicin, idarubicin and idarubicinol with large unilamellar vesicles—Circular dichroism study. *Bba-Biomembranes* **1998**, *1370*, 31–40. [CrossRef]

32. Sangster, J. Octanol-Water Partition-Coefficients of Simple Organic-Compounds. *J. Phys. Chem. Ref. Data* **1989**, *18*, 1111–1229. [CrossRef]

33. Kolitz-Domb, M.; Corem-Salkmon, E.; Grinberg, I.; Margel, S. Synthesis and characterization of bioactive conjugated near-infrared fluorescent proteinoid-poly(L-lactic acid) hollow nanoparticles for optical detection of colon cancer. *Int. J. Nanomed.* **2014**, *9*, 5041–5053. [CrossRef]

34. Joshi, S.; Husain, M.M.; Chandra, R.; Hasan, S.K.; Srivastava, R.C. Hydroxyl radical formation resulting from the interaction of nickel complexes of L-histidine, glutathione or L-cysteine and hydrogen peroxide. *Hum. Exp. Toxicol.* **2005**, *24*, 13–17. [CrossRef] [PubMed]

35. Matthews, J.M.; Sunde, M. Zinc fingers–Folds for many occasions. *IUBMB Life* **2002**, *54*, 351–355. [CrossRef] [PubMed]

36. Michalek, J.L.; Besold, A.N.; Michel, S.L. Cysteine and histidine shuffling: Mixing and matching cysteine and histidine residues in zinc finger proteins to afford different folds and function. *Dalton Trans.* **2011**, *40*, 12619–12632. [CrossRef] [PubMed]

37. Sundberg, R.J.; Martin, R.B. Interactions of histidine and other imidazole derivatives with transition metal ions in chemical and biological systems. *Chem. Rev.* **1974**, *74*, 471–517. [CrossRef]

38. Higuchi, T.; Kotwal, P.M. Complexes of Doxorubicin Exhibiting Enhanced Stability. U.S. Patents 4,246,399 A, 20 January 1981.

39. Barick, K.; Nigam, S.; Bahadur, D. Nanoscale assembly of mesoporous ZnO: A potential drug carrier. *J. Mater. Chem.* **2010**, *20*, 6446–6452. [CrossRef]

40. Ravindran, S.; Ozkan, C.S. Self-assembly of ZnO nanoparticles to electrostatic coordination sites of functionalized carbon nanotubes. *Nanotechnology* **2005**, *16*, 1130. [CrossRef]

41. Jochum, T.; Reddy, C.M.; Eichhöfer, A.; Buth, G.; Szmytkowski, J.; Kalt, H.; Moss, D.; Balaban, T.S. The supramolecular organization of self-assembling chlorosomal bacteriochlorophyll c, d, or e mimics. *Proc. Natl. Acad. Sci. USA* **2008**, *105*, 12736–12741. [CrossRef] [PubMed]

42. Zhang, W.; Song, J.J.; Zhang, B.Z.; Liu, L.W.; Wang, K.R.; Wang, R. Design of Acid-Activated Cell Penetrating Peptide for Delivery of Active Molecules into Cancer Cells. *Bioconj. Chem.* **2011**, *22*, 1410–1415. [CrossRef] [PubMed]

43. Liu, B.R.; Huang, Y.W.; Winiarz, J.G.; Chiang, H.J.; Lee, H.J. Intracellular delivery of quantum dots mediated by a histidine- and arginine-rich HR9 cell-penetrating peptide through the direct membrane translocation mechanism. *Biomaterials* **2011**, *32*, 3520–3537. [CrossRef] [PubMed]

44. Johnson, R.P.; Uthaman, S.; John, J.V.; Lee, H.R.; Lee, S.J.; Park, H.; Park, I.K.; Suh, H.; Kim, I. Poly(PEGA)-*b*-poly(L-lysine)-*b*-poly(L-histidine) Hybrid Vesicles for Tumoral pH-Triggered Intracellular Delivery of Doxorubicin Hydrochloride. *ACS Appl. Mater. Interfaces* **2015**, *7*, 21770–21779. [CrossRef] [PubMed]

45. Bagherifam, S.; Skjeldal, F.M.; Griffiths, G.; Maelandsmo, G.M.; Engebraten, O.; Nystrom, B.; Hasirci, V.; Hasirci, N. pH-Responsive nano carriers for doxorubicin delivery. *Pharm. Res.* **2015**, *32*, 1249–1263. [CrossRef] [PubMed]

46. Wu, H.; Zhu, L.; Torchilin, V.P. pH-Sensitive poly(histidine)-PEG/DSPE-PEG co-polymer micelles for cytosolic drug delivery. *Biomaterials* **2013**, *34*, 1213–1222. [CrossRef] [PubMed]

47. Wu, J.L.; Liu, C.G.; Wang, X.L.; Huang, Z.H. Preparation and characterization of nanoparticles based on histidine-hyaluronic acid conjugates as doxorubicin carriers. *J Mater. Sci. Mater. Med.* **2012**, *23*, 1921–1929. [CrossRef] [PubMed]

48. Upreti, M.; Jyoti, A.; Sethi, P. Tumor microenvironment and nanotherapeutics. *Transl. Cancer Res.* **2013**, *2*, 309–319. [CrossRef] [PubMed]

49. Wang, Y.G.; Zhou, K.J.; Huang, G.; Hensley, C.; Huang, X.N.; Ma, X.P.; Zhao, T.; Sumer, B.D.; DeBerardinis, R.J.; Gao, J.M. A nanoparticle-based strategy for the imaging of a broad range of tumours by nonlinear amplification of microenvironment signals. *Nat. Mater.* **2014**, *13*, 204–212. [CrossRef] [PubMed]

50. Barar, J.; Omidi, Y. Dysregulated pH in Tumor Microenvironment Checkmates Cancer Therapy. *Bioimpacts* **2013**, *3*, 149–162. [CrossRef] [PubMed]

51. Gillies, R.J.; Raghunand, N.; Karczmar, G.S.; Bhujwalla, Z.M. MRI of the tumor microenvironment. *J. Magn. Reson. Imaging JMRI* **2002**, *16*, 430–450. [CrossRef] [PubMed]

52. Danhier, F.; Feron, O.; Preat, V. To exploit the tumor microenvironment: Passive and active tumor targeting of nanocarriers for anti-cancer drug delivery. *J. Control Release* **2010**, *148*, 135–146. [CrossRef] [PubMed]

53. Bhujwalla, Z.M.; Artemov, D.; Ballesteros, P.; Cerdan, S.; Gillies, R.J.; Solaiyappan, M. Combined vascular and extracellular pH imaging of solid tumors. *NMR Biomed.* **2002**, *15*, 114–119. [CrossRef] [PubMed]

Sample Availability: Samples of the compounds are not available from the authors.